

## Recent Aerodynamics Research in the DSTO Water Tunnel

Lincoln P. Erm

Air Vehicles Division, Defence Science and Technology Organisation  
 506 Lorimer Street, Fishermans Bend, 3207 AUSTRALIA

### Abstract

To help meet research requirements at the Defence Science and Technology Organisation, new testing capabilities have been developed for an existing water tunnel. A low-load-range two-component strain-gauge-balance system has been developed to measure normal forces and pitching moments on models. A dynamic-testing capability has also been developed, that enables loads and images of the flow to be acquired while a model is in motion, undergoing a dynamic manoeuvre in roll, pitch and yaw. Details of the upgraded facility, together with some test results obtained using a 70° delta wing, are given in this paper.

### Notation

$C_m$	Pitching-moment coefficient, $C_m = m/(0.5\rho U^2 S \bar{c})$ .
$C_N$	Normal-force coefficient, $C_N = Z/(0.5\rho U^2 S)$ .
$c$	Root chord of a delta wing, (m), $c = 0.3$ m.
$\bar{c}$	Mean aerodynamic chord (mac) of a delta wing, (m).
$f$	Equivalent constant circular frequency of rotation, (Hz).
$k$	Reduced frequency of oscillation, $k = \pi f \bar{c} / U$ .
$l, m, n$	Rolling, pitching and yawing moments respectively for the wing and balance coordinate systems, (N.m).
$S$	Plan-view projected area of the wing at $\alpha = 0^\circ$ , (m <sup>2</sup> ).
$t$	Time from the start of a dynamic manoeuvre, (s).
$U$	Free-stream velocity in test section of tunnel, (m/s).
$X, Y, Z$	Axial, side and normal forces respectively for the wing and balance coordinate systems, (N).
$x, y, z$	Axes for the wing and balance coordinate systems.
$\alpha$	Angle of attack, (deg).
$\alpha_0$	Mean angle of attack, (deg) (used in dynamic tests).
$\rho$	Density of a fluid, (kg/m <sup>3</sup> ).

### Introduction

Vortex flows over modern combat aircraft during advanced manoeuvring are extremely complex, being unsteady, three-dimensional and highly non-linear, with separations, reattachments and vortex breakdowns. At the Defence Science and Technology Organisation (DSTO), there is a need to improve the understanding of the physics of such flows, and the way in which they affect loads on aircraft. Research work can be carried out to a limited extent using full-size aircraft, but this is costly and it is often difficult to obtain the required flight conditions in an atmospheric environment. It is generally necessary to carry out the research using models in tunnels, which is far cheaper and where there is greater control over operating conditions.

Wind tunnels are primarily used to measure forces and moments on models, as larger models and higher free-stream velocities are used compared with water tunnels. Water tunnels are better suited to flow-visualization studies, due to water having a higher density and lower mass diffusivity than air, and because free-stream velocities used in water tunnels are usually much lower than those in wind tunnels. Images of the flow captured in water tunnels are detailed, but the forces and moments on models in small water tunnels, like the one at DSTO, are very low and they have not been able to be measured accurately in the past. If the low loads could be measured accurately, then they could be directly correlated with the detailed flow patterns, which would

provide an insight into how physical aspects of the flow affect the loads. Another advantage of testing in water tunnels is that the required rotation rate to simulate a scaled dynamic manoeuvre is over 100 times smaller than that for a wind tunnel, so that the effects of model inertia on the measured loads are negligible.

With recent developments in strain-gauge technology, measuring small forces and moments on models in water tunnels is now a viable option. This has led to the development of a two-component strain-gauge-balance system to measure flow-induced normal forces and pitching moments on models in the DSTO water tunnel. A dynamic-testing capability has also been developed for the tunnel, enabling loads and images of the flow to be acquired while a model is undergoing a dynamic manoeuvre in roll, pitch and yaw. Details of the new testing capabilities, together with some test results obtained using a 70° delta wing, are given in this paper.

### DSTO Water Tunnel

The DSTO water tunnel was made by Eidetics International Incorporated (now called Rolling Hills Research Corporation), and is designated Model 1520. The tunnel, shown in figure 1, has a horizontal-flow test section 380 mm wide, 510 mm deep and 1630 mm long, with walls made from glass to facilitate flow-visualisation studies. It is a closed circuit continuous-flow tunnel with a free surface in the test section. The free-stream velocity can be varied between 0 and 0.6 m/s. Models are mounted on a C-strut so that the centre of rotation of a model is at the centre of the imaginary circle formed by the strut. Further details of the tunnel are given by Erm [3].

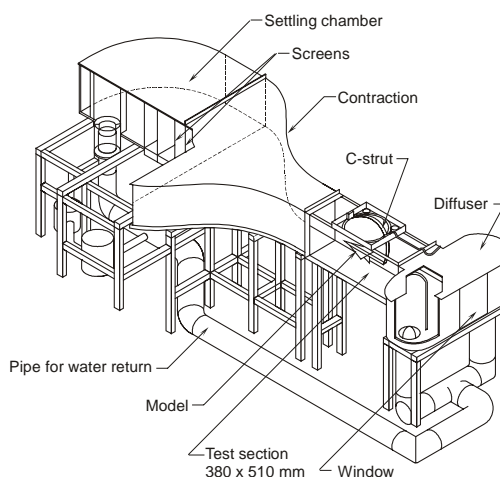


Figure 1. Eidetics Model 1520 water tunnel.

### Development of a Strain-Gauge-Balance System

A strain-gauge-balance system has been developed for measuring flow-induced normal forces and pitching moments on a model in the water tunnel. The system is comprised of a low-load-range two-component balance, a signal-conditioning system and a PC-controlled data-acquisition system. Full details of the system are given by Erm [3].

For the DSTO water tunnel operating at a free-stream velocity of 0.1 m/s, flow-induced forces and moments on models are very small, being typically within the ranges  $\pm 2.5$  N and  $\pm 0.02$  N.m respectively. For comparison, the loads on models in the low-speed wind tunnel at DSTO are typically within the ranges  $\pm 3500$  N and  $\pm 300$  N.m respectively. There is a factor of 1400 for normal forces and 15000 for pitching moments between the loads on models in the two tunnels.

A diagrammatic representation of the balance is given in figure 2. The right-handed orthogonal coordinate system remains fixed to the balance, with the origin located on the longitudinal axis at the geometric centre of the gauges. For completeness, the full conventional set of axes and loads are given, but the balance can only measure normal forces ( $Z$ ) and pitching moments ( $m$ ). Due to the small flow-induced loads, semi-conductor strain gauges have been used, having a resistance of 1000  $\Omega$ , a gauge factor of 145, and active dimensions of 1.27 mm long by 0.15 mm wide. The balance contains four gauges on each of the two sides of the flexure member, and the gauges have been wired together to form Wheatstone bridges for the two circuits. The gauges and the connecting leads have been waterproofed by coating them with a silicone-rubber compound. The balance was calibrated manually using a conventional deadweight procedure. Normal forces and pitching moments can be measured to within  $\pm 0.8\%$  and  $\pm 0.3\%$  of their true values respectively.

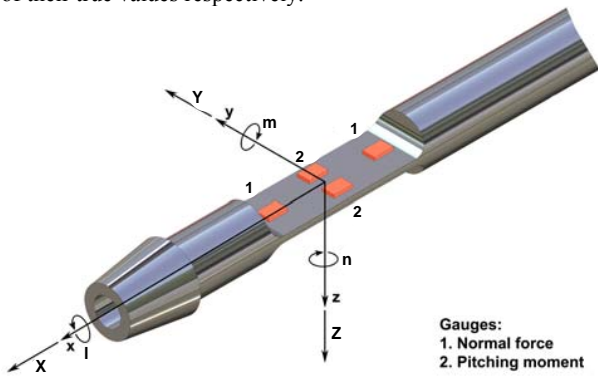


Figure 2. Two-component balance, showing the position of the gauges for the normal-force and pitching-moment circuits

### Experimental Results: Static Forces and Moments

Flow-induced normal forces and pitching moments were measured on the delta wing shown in figure 3. The wing is made of Perspex and it was painted matt black. It has a root chord of 300.0 mm, a span of 218.4 mm, a thickness of 6.5 mm, and the leading-edge sweep angles are  $70^\circ$ . The edges of the wing are square to the leeward surface for the first 0.5 mm from that surface, and they are then bevelled at  $30^\circ$  for the remaining 6 mm of the thickness, as shown. The mean aerodynamic chord ( $\bar{c}$ ) is  $2/3$  of the root chord i.e.  $\bar{c} = 200.0$  mm. A metal tubular insert is embedded in the wing along its centreline to accommodate the balance, which was positioned so that the origin of its coordinate system was located at the 50%  $\bar{c}$  position.

Normal forces and pitching moments were measured for fixed values of  $\alpha$  varying from  $0^\circ$  to  $60^\circ$ , in increments of  $2^\circ$ , for  $U = 0.1$  m/s. Values of  $C_N$  are shown in figure 4 and corresponding values of  $C_m$ , referenced to the 30%, 40% and 50%  $\bar{c}$  positions (see figure 3) are shown in figure 5. Each experimental point for the DSTO data shown in figures 4 and 5 corresponds to an average of 50 sets of gauge output voltages, sampled at an interval of 1 s per set. DSTO data have been corrected for the effects of tunnel blockage using the corrections proposed by Cunningham & Bushlow [2].

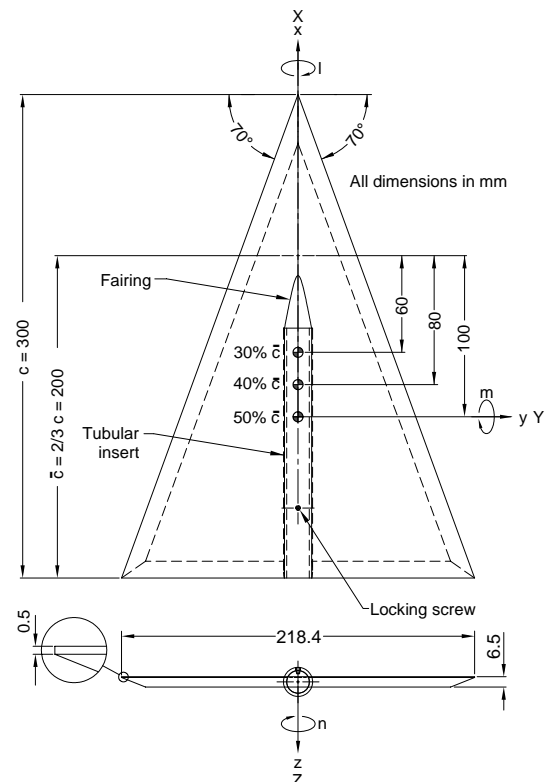


Figure 3. Delta wing used at DSTO

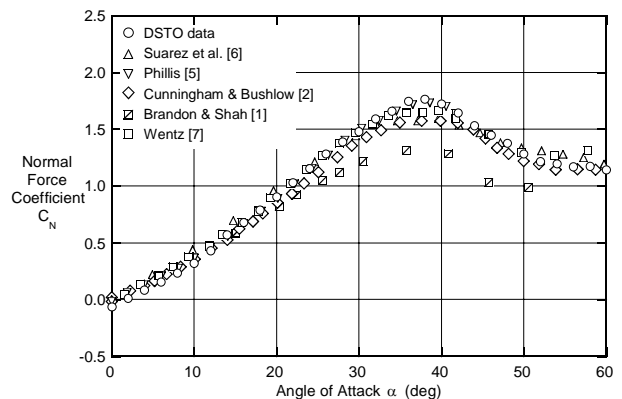


Figure 4. Normal-force coefficients for the DSTO delta wing compared with data obtained by other researchers.

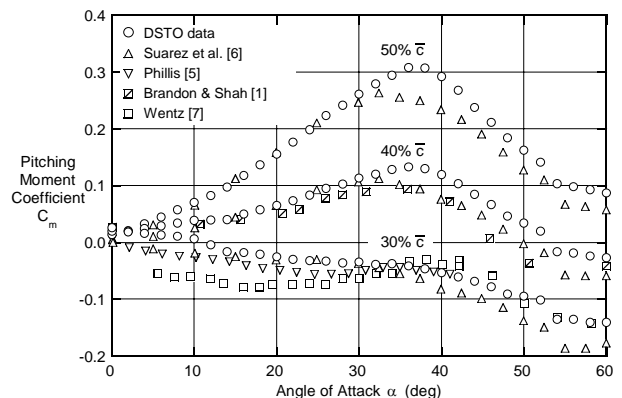


Figure 5. Pitching-moment coefficients for the DSTO delta wing compared with data obtained by other researchers.

The DSTO  $C_N$  and  $C_m$  measurements taken on the  $70^\circ$  delta wing are compared in figures 4 and 5 with similar measurements taken on  $70^\circ$  delta wings in other tunnels.  $C_N$  data are compared, in

figure 4, with those of Suárez *et al.* [6] (water tunnel), Phillis [5] (wind tunnel), Cunningham & Bushlow [2] (water tunnel), Brandon & Shah [1] (wind tunnel) and Wentz [7] (wind tunnel). Corresponding DSTO  $C_m$  data, computed for different moment reference centres, which match the reference centres used by these researchers, are compared in figure 5. There is good agreement between the DSTO data and that given by other researchers. Variations between the different sets of data could be due to differences in Reynolds numbers, flow quality, flow blockage, or differences in the leading edges of the wings. For example, the leading edges of the DSTO wing were only bevelled on one side (see figure 3), whereas those on the wing used by Suárez *et al.* [6] were bevelled on both sides.

### Development of a Dynamic-Testing Capability

A dynamic-testing system has been developed for the water tunnel that enables flow-induced forces and moments on a model to be measured and images of the flow to be captured while it is in motion undergoing a predetermined dynamic manoeuvre in roll, pitch and yaw. The operation of the dynamic rig is controlled using dedicated software. Acquisition of data has been synchronised so that loads and images are acquired simultaneously throughout a manoeuvre at fixed instants of time corresponding to known model orientations. Further details of the dynamic rig are given by Erm [4].

The setup of the upgraded model-motion system is shown in figure 6. Roll, pitch and yaw angles can be varied between  $0^\circ$  and  $\pm 360^\circ$ ,  $-20^\circ$  and  $55^\circ$ , and  $-20^\circ$  and  $+20^\circ$  respectively. The maximum obtainable roll, pitch and yaw rotational speeds of a model are 12, 6 and 8 deg/s respectively.

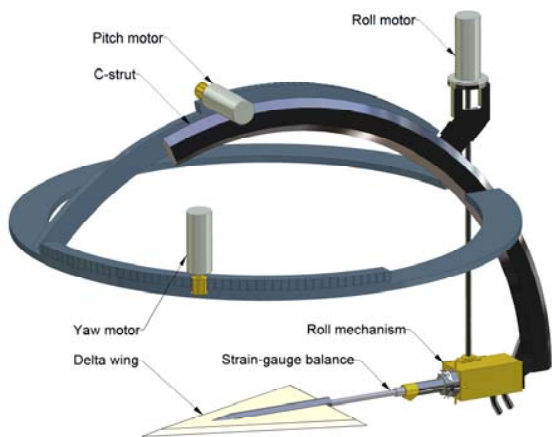


Figure 6. Upgraded model-motion system.

A graphical-user interface is used to set the tunnel free-stream velocity, to control the on/off switches for the dye-flow pump, to control the model motion, to sample voltages corresponding to forces and moments on a model, and to control the capture of images of the flow using digital video cameras. The interface has the general form shown in figure 7. Throughout a dynamic test, the interface can display instantaneous information including roll, pitch and yaw angles of the model, tunnel free-stream velocity and balance output voltages.

At the completion of a dynamic run, the sampled data can be examined using dedicated software. Images of the flow throughout a manoeuvre can be played back and corresponding (1) instants of time, (2) tunnel free-stream velocities, (3) model roll, pitch and yaw angles, and (4) forces and moments on the model, are imprinted on each image. It is therefore possible to assess directly how loads on the model are affected by different types of flow patterns over the model.

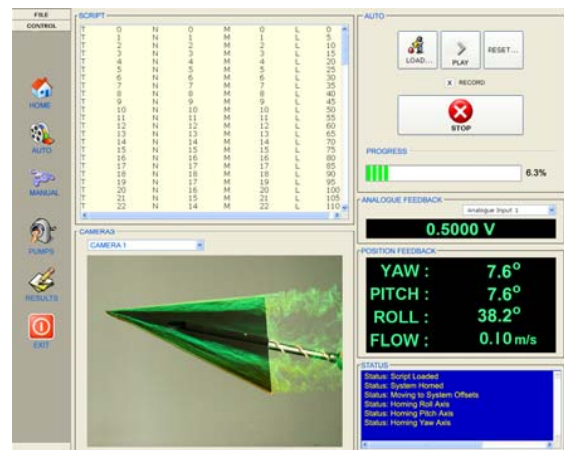


Figure 7. Graphical-user interface used when carrying out tests.

### Experimental Results: Static and Dynamic Forces and Moments

Flow-induced normal forces and pitching moments were measured on the delta wing when it was undergoing oscillatory pitching motions. To enable the DSTO dynamic data to be compared with the water-tunnel data of Suárez *et al.* [6], the sinusoidal pitching motions used for the DSTO tests were chosen to be similar. For Suárez *et al.*,  $k = \pi f \bar{c} / U$  had a value of 0.0376 and their wing was oscillated with simple harmonic angular motion about four different mean values of  $\alpha$ , viz.  $\alpha_0 = 22^\circ, 27^\circ, 32^\circ$  and  $37^\circ$ , varying by  $\pm 18^\circ$  from each of the four values of  $\alpha_0$ . For the DSTO tests,  $k$  was 0.0376,  $\bar{c}$  was 0.200 m and  $U$  was 0.1 m/s, so that  $f$  was 0.00598 Hz, corresponding to a time of 167.1 s for a full cycle.

DSTO  $C_N$  data are compared with those of Suárez *et al.* [6] in figure 8 and corresponding  $C_m$  data, for the 50%  $\bar{c}$  reference position, are compared in figure 9. The DSTO dynamic data are the average of 3 dynamic runs. The DSTO dynamic measurements and those obtained by Suárez *et al.* [6] have virtually the same magnitudes and show very similar trends. The reasons for the relatively small differences between the two sets of data could be the same as those given above for the static data.

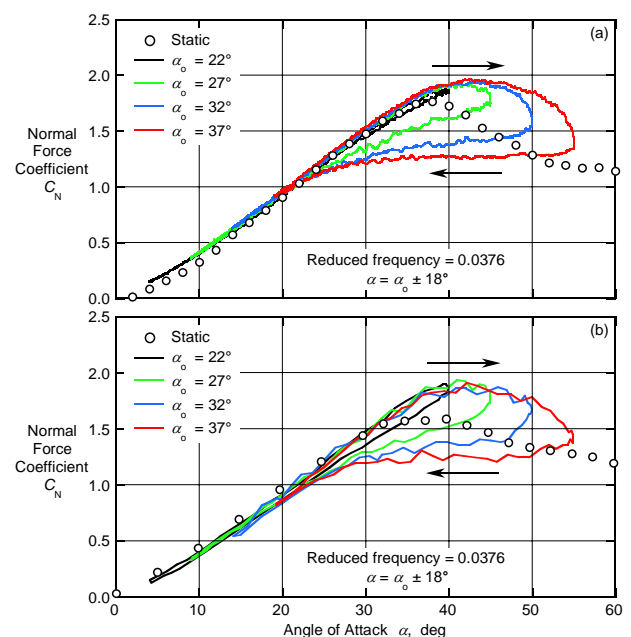


Figure 8. Normal-force coefficients for the DSTO delta wing compared with corresponding data obtained by Suárez *et al.* [6]. (a) DSTO data, (b) data of Suárez *et al.*

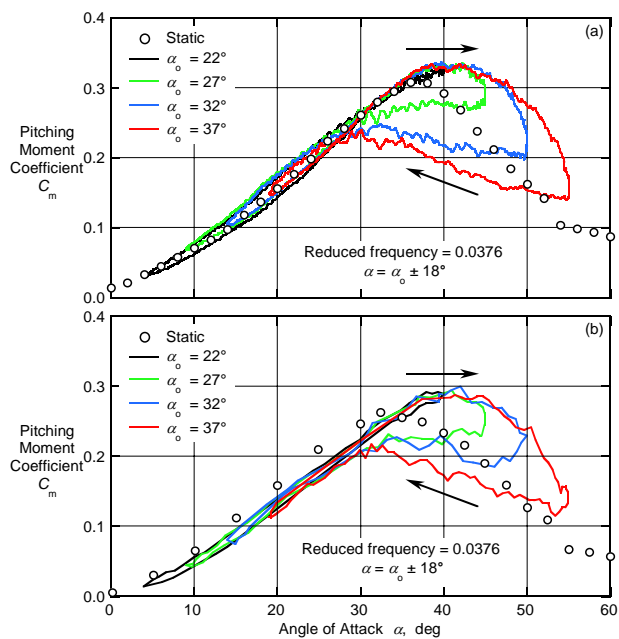


Figure 9. Pitching-moment coefficients for the DSTO delta wing compared with corresponding data obtained by Suárez et al [6]. (a) DSTO data, (b) data of Suárez *et al.*

### Experimental Results: Static and Dynamic Flow Images

During the foregoing tests, the flow was visualized to gain an insight into how it was affected by the motion. The flow is dominated by two large bound counter-rotating vortices on the leeward surface, formed by the rolling up of the flow that separates along the leading edges of the wing. The vortices were visualized using sodium fluorescein dye injected from a single metal tube attached to the windward surface of the wing and having its outlet close to the apex. The dye from the tube divided into two streams, which passed into the cores of the vortices.

Figure 10 shows an image of the flow when the wing was stationary and set at  $\alpha = 32^\circ$ , as well as images when it was undergoing sinusoidal pitching motion about  $\alpha_0 = 32^\circ$ , varying by  $\pm 18^\circ$  from  $\alpha_0$ , with  $k = 0.0376$ . Each image in figure 10 corresponds to  $\alpha = 32^\circ$ , but  $\alpha$  is increasing in figure 10a,  $\alpha$  is fixed in figure 10b and  $\alpha$  is decreasing in figure 10c.

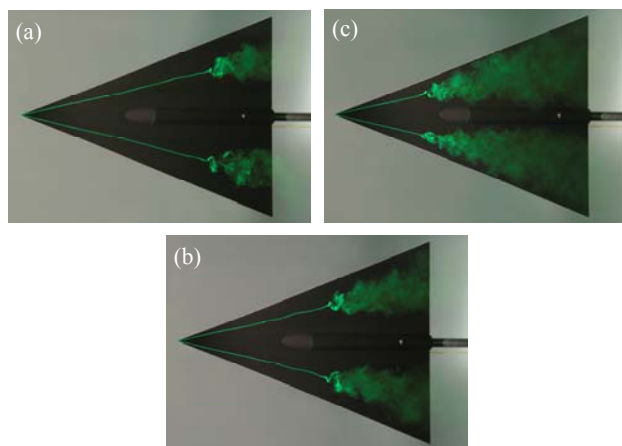


Figure 10. Flow over a delta wing, pitching tests,  $\alpha = 32^\circ$ . (a) increasing  $\alpha$ , (b) static, (c) decreasing  $\alpha$ .

For increasing  $\alpha$ , the breakdown regions are moving towards the apex and conversely for decreasing  $\alpha$ . For both cases of the wing passing through  $\alpha = 32^\circ$ , the flow structure is moving towards the condition for the wing stationary at  $\alpha = 32^\circ$ . For increasing  $\alpha$ ,

the motion of the wing into the body of water on the leeward side tends to push the vortices towards the wing surface, which increases the lift, due to greater suction caused by higher velocities, and conversely for decreasing  $\alpha$ . During oscillatory pitching motion, the lag in the movement of the breakdown region and the movement of the vortices towards or away from the surface affects the aerodynamic loads on the wing, which caused the hysteresis loops shown in figures 8a and 9a.

### Concluding Remarks

New testing capabilities have been developed for the water tunnel at DSTO. A two-component strain-gauge-balance system has been developed to measure the very small flow-induced normal forces and pitching moments on models. The balance uses semiconductor strain gauges and is capable of measuring normal forces and pitching moments up to  $\pm 2.5$  N and  $\pm 0.02$  N.m respectively. A dynamic-testing system has also been developed for the tunnel that enables flow-induced forces and moments on a model to be measured and images of the flow to be captured while it is in motion, undergoing a manoeuvre in roll, pitch and yaw. Model motion and data acquisition is controlled via a PC, using dedicated software. Data acquisition has been synchronized so that forces and moments, images of the flow, and the roll, pitch and yaw angles, are all acquired for the same instants of time throughout a dynamic manoeuvre. The loads can therefore be directly correlated with the detailed flow patterns.

The upgraded facility was used to carry out tests using a sharp-edged  $70^\circ$  delta wing. Measured flow-induced normal forces and pitching moments agreed well with published data, showing that the rig gives credible results, at least for a sharp-edged delta wing, where large-scale flow patterns are generally independent of Reynolds number. Further research needs to be carried out to confirm the utility of the water-tunnel facility in generating aerodynamic data for non-sharp leading-edge geometries.

### Acknowledgments

The author is grateful for the help given by Neil Matheson, Owen Holland, Phil Ferrarotto, Michael Konak, Chris Jones, John Clayton, Kevin Desmond and Alberto Gonzalez.

### References

- [1] Brandon, J. M. & Shah, G. H., Effect of large amplitude pitching moments on the unsteady aerodynamic characteristics of flat-plate wings, Paper 88-4331-CP, *AIAA Atmospheric Flight Mechanics Conference*, Minneapolis, MN, USA, 15-17 Aug. 1988.
- [2] Cunningham, A. M. Jr. & Bushlow, T., Steady and unsteady force testing of fighter aircraft models in a water tunnel, Paper 90-2815-CP, *AIAA 8th Applied Aerodynamics Conference*, Portland, OR, USA, 20-22 Aug. 1990.
- [3] Erm, L. P., Development of a two-component strain-gauge-balance load-measurement system for the DSTO water tunnel, *DSTO-TR-1835*, Defence Science and Technology Organisation, Melbourne, Australia, Mar. 2006.
- [4] Erm, L. P., Development and use of a dynamic-testing capability for the DSTO water tunnel, *DSTO-TR-1836*, Defence Science and Technology Organisation, Melbourne, Australia, Mar. 2006.
- [5] Phillis, D. L., Force and pressure measurements over a  $70^\circ$  delta wing at high angles of attack and sideslip, Masters Thesis, Aeronautical Engineering Department, The Wichita State University, USA, 1991.
- [6] Suárez, C. J., Malcolm, G. N., Kramer, B. R., Smith, B. C. & Ayers, B. F., Development of a multicomponent force and moment balance for water tunnel applications, Volumes I and II, *NASA Contractor Report 4642*, 1994.
- [7] Wentz, W. H. Jr., Wind tunnel investigations of vortex breakdown on slender sharp-edged wings, PhD Dissertation, University of Kansas, Lawrence, KS, USA, 1969.